Novel RF Front End Designs Based on Active Integrated Antenna Concepts

Sang-Min Han, Younkyu Chung[1], and Tatsuo Itoh

Abstract — **In this paper recent developments of RF front-end system based on the active integrated antenna design concepts are presented. Thanks to the enhancements in the design of special antennas working as radiator as well as providing the other circuit functionalities, the antenna-integrated RF front ends have been capable of improving the circuit-efficiency and compactness. These enhancements are illustrated in this paper with an AlGaN/GaN HFET power amplifier for a transmitting system and a rectenna for a receiving system.**

Keywords — **Active Integrated Antennas, Circular Sector Antennas, Power Amplifiers, Rectifying Antennas**

I. INTRODUCTION

Active integrated antennas (AIA's) have been provided noble design technologies in modern RF/microwave system architectures for both military and commercial applications. The AIA can be regarded as an active microwave circuit in which the output or input port is free space instead of a conventional 50-Ω interface. In these points of the antenna, special roles such as resonating, filtering, and diplexing, as well as a radiating element are played in a system circuitry. A typical AIA consists of active devices such as Gunn diodes or three-terminal devices to form an active circuit, and planar antennas such as dipoles, microstrip patches, bowties, or slot antennas [1].

Many types of planar antennas such as quasi-Yagi [2]-[5], slot [6], and circular sector antennas [7] have been utilized for AIA applications. The demonstration of the use of the planar quasi-Yagi antennas, which have an extremely wide bandwidth of 50% with lower front-back ratio and cross polarization, were successfully accomplished [2]-[5]. In [3], the antenna was integrated with a push-pull power amplifier configuration to terminate the second harmonic providing higher power efficiency. It was also used for a LNA in monopulse radar applications [4]. In addition to the amplifier applications, the antenna was also applied to a subharmonic balanced 60-GHz self-oscillating mixer [5]. The elimination of a local oscillator (LO) leads to a very simple receiver. Therefore the antenna can provide the radiation and anti-phase power combination as well as the harmonic termination.

S.-M. Han and T. Itoh are with the Department of Electrical Engineering, University of California, Los Angeles, 405 Hilgard Ave., Los Angeles, CA 90095 USA, E-mail: smhan@ee.ucla.edu, itoh@ee.ucla.edu).
[1]Y. Chung was with UCLA. Now he is with California Institute of Technology, E-mail: ykchung@caltech.edu.

A dual-feed slot and a circular sector antenna were utilized for the high efficiency power amplifiers in [6]-[7]. The antennas reflect high order harmonics back to the active transistors, resulting in high efficiency performance. In particular, the circular sector antenna achieves the harmonic rejection characteristics with a circular sector angle of 240 ° and a feed angle of 30 ° from the edge of the antenna [8]-[9]. The circular antenna has also been used for a rectifying antenna (rectenna) to obtain higher efficiency as well as to reduce circuit complexity [9]-[10].

In this paper, two RF front-end subsystems integrated with a circular sector antenna, which characterizes the harmonic rejection, are introduced. By means of the use of such an antenna with a special circuit functionality, a high power amplifier can be designed with the antenna in a transmitting circuit, because it requires re-use of harmonic power generated by non-linear operating transistor. A rectenna also needs to block re-radiation of harmonic signals to increase conversion efficiency in a receiving circuit. These circuitries have been designed by the AIA design technologies without impedance matching circuits or bandpass filters (BPFs).

II. AlGaN/GaN HFET HIGH EFFICIENCY POWER AMPLIFIER

A. Development of High Power Amplifiers

Over the past years, high efficiency power amplifiers have been investigated and realized via controlling higher order output harmonics from the nonlinear active device [11]-[14]. High efficiency operation ideally occurs when the harmonics of the output voltage have the right magnitudes and phases to form a square wave. This effect can be realized by placing short circuits at the even harmonics and open circuits at the odd harmonics [12]-[13]. Specifically, the second harmonic is designed to be short-circuited while the third harmonic is open-circuited, making the drain voltage waveform of a FET transistor closer to a square wave form. High efficiency was achieved by terminating higher order harmonics reactively so that only fundamental signal power is delivered to the output load, while other higher order harmonics are reflected reactively. When the power amplifier is connected with a transmitter antenna, most of these widely used design methodologies inevitably suffer from cable or feedline losses. For the power amplifier which is operating at the saturated output power range, the loss of even a small amount of power from the cable or feedline degrades the total system efficiency. For high performance RF front-end applications, a new power

amplifier design methodology based on the AIA design concept has been proposed and demonstrated [15]-[16].

Recently, high performance RF front-end circuits using the AIA design concept have been reported. Deal *et al* demonstrated AIA push-pull GaAs FET power amplifiers at 2.5 GHz and 2.46 GHz. Peak PAEs of 55 % and 63 % were demonstrated at 25 dBm and 26 dBm output powers, respectively [15]. Radisic *et al* showed high efficiency GaAs FET amplifier for wireless applications. A maximum PAE of 63 % and output power of 24.4 dBm were reported at 2.55 GHz [16]. Hang *et al* presented GaAs FET push-pull power amplifier with 60.9 % peak PAE and 28.2 dBm output power at 4.15 GHz [3]. Unlike AIAs with a commercial GaAs-based FET presented in the literature [3],[15]-[16], when a commercial large-signal device model is not available, the large-signal behavior of a FET has to be accurately characterized to maximize PAE and output power. As an empirical technique, load-pull measurement has been successfully used for this purpose [17].
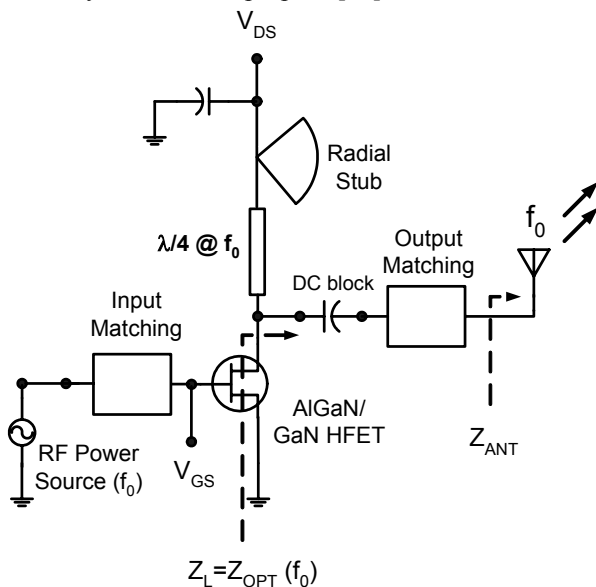
Fig. 1 Schematic of the AlGaN/GaN HFET power amplifier integrated with microstrip antenna as a RF front-end application. Measured antenna impedance (Z_{ANT}) is directly transformed to optimum load impedance (Z_{OPT}) for efficiency.

B. Circuit Design and Fabrication

In this work, the AlGaN/GaN HFET power amplifier integrated with antenna as shown in Fig. 1 is demonstrated for high efficiency and compact RF front-end applications. Based on the AIA design concept, the measured passive antenna impedance (Z_{ANT}) is directly transformed to the optimum load impedance (Z_{OPT}) for maximum efficiency. The power amplifier was designed at 7.25 GHz using Agilent Technologies' ADS simulator. A load-pull measurement to extract Z_{OPT} from the HFET with 1mm gate periphery and 0.25 μm gate length was done using the Maury Microwave load-pull measurement setup. For the load-pull measurement, bias voltages were set as V_{DS} = 18 V and V_{GS} = -5 V. This

corresponds to 10 % of the I_{DSS}, achieving high power added efficiency (PAE) while keeping relatively high gain and high output power. The measured load-pull large-signal performance for a 1 mm-wide device is shown in Fig. 2. The saturated output power reaches 31.7 dBm. The associated power gain of 8.7 dB and peak PAE of 45 % are observed.
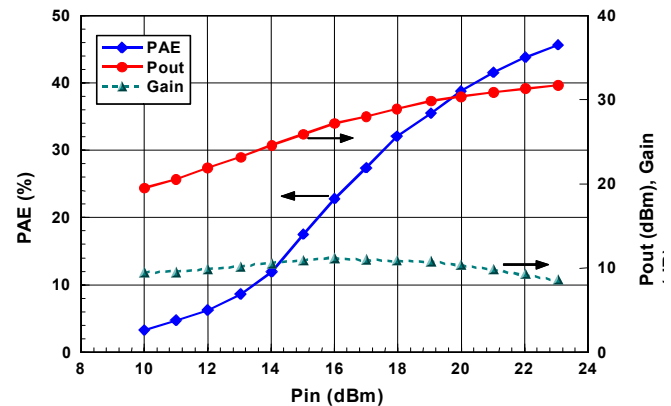
Fig. 2 Measured load-pull large-signal performance for a 1 mm-wide AlGaN/GaN HFET.
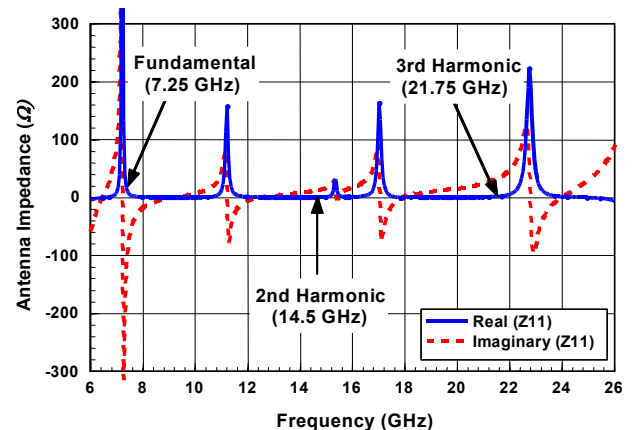
Fig. 3 The resonant characteristic of the microstrip circular sector antenna on RT/Duroid substrate with dielectric constant of 10.2 and thickness of 10 mils ($Z_{11}=Z_{ANT}$).

The microstrip circular sector antenna with a 120° cut-out has the interesting characteristic not to exhibit radiating modes at higher order harmonics of the first resonant frequency [16]. The cut-out circular sector antenna thus provides an efficient way to suppress higher order harmonic power as compared to a rectangular type patch antenna. The microstrip circular sector antenna was designed at 7.25 GHz operating frequency which is slightly off the exact resonant frequency, enabling easy output matching to avoid the high impedance at the exact resonant frequency. The designed antenna was fabricated on Duroid substrate with dielectric constant of 10.2 and thickness of 10 mils. The resonant characteristic of the microstrip circular sector antenna is shown in Fig. 3. Clearly, no power radiation characteristic at higher order harmonics is observed from the Z_{ANT} in Fig. 3. Then, the Z_{ANT} was embedded into the simulator as one-port data at the final output terminal instead of a 50-Ω load in the design of the conventional amplifiers.

Because the output matching is critical in determining the output power and efficiency, the circuit design was carefully done. In this work, the measured Z_{ANT} is directly transformed to the Z_{OPT} for optimum efficiency at the fundamental frequency, bypassing the conventional intermediate 50-Ω line stage. No additional output matching network is needed to tune higher order harmonics due to the intrinsic harmonic termination characteristics of the antenna. Thus, the signal power at the fundamental frequency is radiated through the antenna while signal power at higher order harmonics is not due to the reactive termination. The designed output matching network including bias circuit was fabricated on the RT/Duroid substrate with dielectric constant of 10.2 and thickness of 10 mils.

The input matching circuit was designed to transform the low gate impedance of the HFET to 50-Ω, the same as done in the design methodology of conventional amplifiers. The input matching circuit was built on the Alumina substrate with a dielectric constant of 9.8 and thickness of 15 mils. The fabricated individual input and output matching integrated with antenna as well as the AlGaN/GaN HFET were combined and mounted on a test jig. The metal fixture efficiently dissipates heat generated from the AlGaN/GaN HFET so that accurate power performance measurements can be made. We have also considered the effect of the Au bonding wire by factoring in an equivalent inductance [14]. A photograph of the fabricated AlGaN/GaN HFET power amplifier integrated with the microstrip circular sector antenna is shown in Fig. 4.
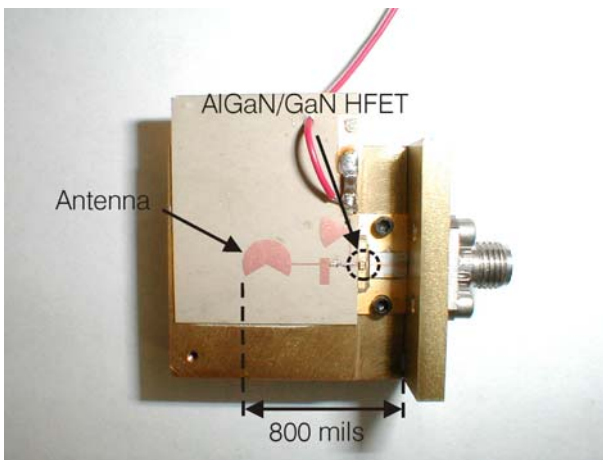
Fig. 4 Photograph of the AlGaN/GaN HFET power amplifier integrated with the microstrip circular sector antenna on the test jig.

C. Experimental Results and Discussion

Because the circuit is terminated with a radiator rather than 50-Ω load, the measurement of this circuit is much more complicated when compared to a standard active circuit. To correctly evaluate the output performance of the power amplifier integrated antenna, care must be taken to calibrate the measurement setup systematically. Employing the Friis transmission equation (1), the measurements in an anechoic chamber have been done in the following order [15]-[16]: First, to de-embed the antenna gain and mismatch loss, measurement of the passive microstrip circular sector antenna as a reference is done in the broadside direction. The passive antenna is then replaced by the power amplifier integrated with the same type of antenna and the measurement is repeated in the same direction. While compensating for the measured mismatch loss and the antenna gain from the measurement data of the passive antenna, all output performance of the power amplifier is correctly obtained. Note that for all of these measurements, the cable loss and receiving antenna gain are accounted for.

$$P_{rec} = \left(1 - |\Gamma_{trans}|^2\right) G_t \frac{P_{av\_HFET}}{4\pi R^2} \left(1 - |\Gamma_{rec}|^2\right) \frac{\lambda^2}{4\pi} G_r \qquad (1)$$

In equation (1), P_{rec} is the power received by the spectrum analyzer and P_{av_HFET} represents the available power from the output of the HFET. Γ_{trans} and Γ_{rec} are reflection coefficients of transmitting and receiving antennas to quantify the mismatch losses, respectively. By considering both P_{av_HFET} and transmitting reflection coefficient, the delivered power to the antenna can be obtained as the output power of AlGaN/GaN HFET power amplifier. In addition, G_t and G_r are transmitting and receiving antenna gain and $1/4\pi R^2$ represents free space loss.
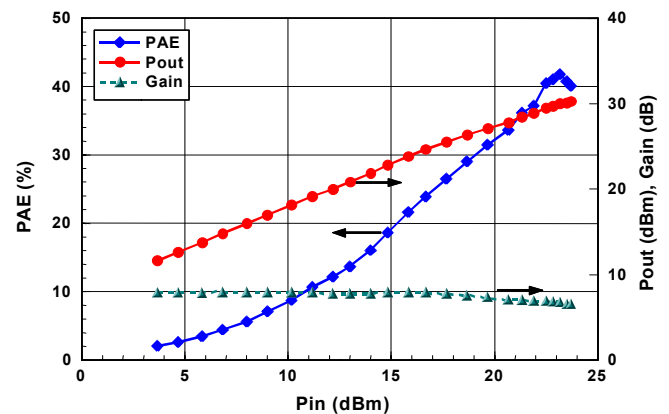
Fig. 5 Measured large-signal performance with respect to input power at 7.25 GHz (V_{DS}=18 V and V_{GS}=-5 V).
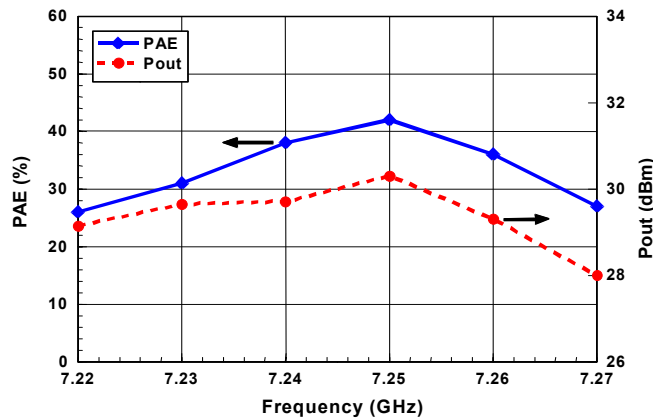
Fig. 6 Measured large-signal performance as a function of frequency for the AlGaN/GaN HFET power amplifier integrated with the microstrip circular sector antenna (V_{DS}=18 V, V_{GS}=-5 V, and P_{in}=23 dBm).
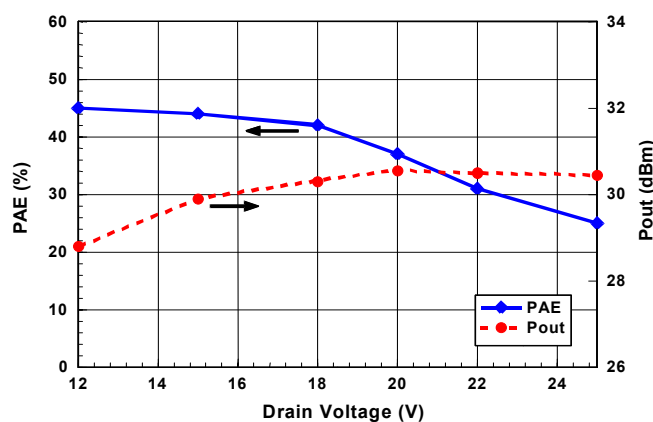
Fig. 7 Measured large-signal performance versus drain bias voltage at 7.25 GHz for the AlGaN/GaN HFET power amplifier integrated with the microstrip circular sector antenna (P_{in}=23 dBm).

Based on the measurement technique, large-signal measurements for the antenna integrated AlGaN/GaN HFET power amplifier mounted on the test jig were performed in the anechoic chamber using a microwave synthesizer in conjunction with a microwave amplifier as a power source to provide sufficient drive power. A spectrum analyzer was used to monitor oscillations over the entire frequency range during the measurement to confirm the stability of the power amplifier. The HFET was first biased at V_{DS} of 18 V and V_{GS} of -5 V, the same as in the load-pull measurement bias setup. In Fig. 5, the measured PAE, output power, and gain are shown as a function of input power for the power amplifier at 7.25 GHz. Peak PAE of 42 % at an input power level of 23 dBm and 30.3 dBm output power with 8 dB linear gain are observed. Compared to measured load-pull data shown in Fig. 2, the deviation can be contributed to circuit fabrication variation such as imperfections in etching of matching circuits and connections. The large-signal performance with respect to frequency is shown for the power amplifier in Fig. 6. Peak PAE from 26 % to 42 % is observed for output power ranging from 28 dBm to 30.3 dBm output power at an input power of 23 dBm. The relatively narrow frequency bandwidth can be explained by the resonant characteristic of the microstrip

circular   sector   antenna,

(a)

(b)
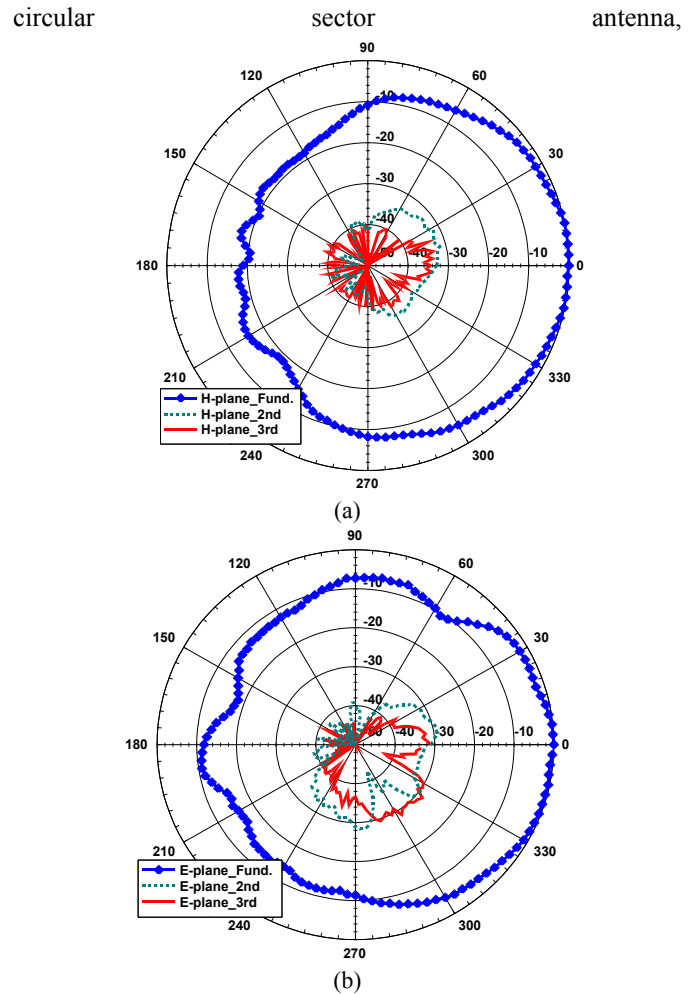
Fig. 8 Measured radiation patterns at the fundamental of 7.25 GHz, second, and third harmonic frequencies for the AlGaN/GaN HFET power amplifier integrated with the microstrip circular sector antenna. (a) H-plane. (b) E-plane.

which ideally radiates at single designed resonant frequency. In Fig. 7, the V_{DS} dependent large-signal performance of the power amplifier at 7.25 GHz and 23 dBm input driving power is shown. Output power continues to increase up to 30.5 dBm at 25 V while efficiency decreases because of high DC power consumption. 45 % peak PAE is observed at 15 V.

High efficiency power amplifiers which are normally biased at class-AB or class-B generate substantial higher order harmonics. For the antenna integrated power amplifier, these harmonics can radiate out through the antenna and overall system performance can be significantly degraded by these undesired higher order harmonics. In this work, high efficiency performance has been realized via suppression of the higher order harmonics by employing the microstrip circular sector antenna. The higher order harmonic suppression characteristics of the power amplifier can be observed by measuring the second and third harmonic radiation. Fig. 8 show the H- and E-plane radiation patterns at fundamental, second, and third harmonics, respectively. The measurement was done at the input power level corresponding to the peak PAE and the maximum power was normalized to 0 dB. As shown in Fig. 8, second and third harmonic suppression better than 30 dB has

been measured in both the H- and E-planes. Note that in this measurement, output power levels at all the frequencies were referred to the reference plane at the output of the AlGaN/GaN HFET power amplifier. This is done by taking into account the cable and free space losses, receiving antenna gain, and mismatch loss at the corresponding frequencies.

The compactness of the implemented AlGaN/GaN HFET power amplifier integrated with the microstrip circular sector antenna is realized by employing 10.2 high dielectric constant substrate as well as the AIA design approach which eliminates the unnecessary connecting components between power amplifier and antenna in conventional transmitters. As GaN-based device technology matures, a power amplifier integrated with an antenna or a transmitter in next generation wireless systems will be able to be integrated together on sapphire substrate with high dielectric constant of 11.6 in parallel and 9.4 in perpendicular direction. This MMIC design reduces circuit size through the high dielectric sapphire substrate providing large size wafer growth at lowered costs [18].

III. RECTENNA INTEGRATED WITH A CIRCULAR SECTOR ANTENNA

A. Rectenna Based Upon the AIA Concept

In order to transmit power without wires, the rectifying antenna (rectenna) which converts RF power to DC power has been researched [19]-[21]. The rectenna system consisting of a receiving antenna, matching circuits, a BPF, a diode, and a lowpass filter (LPF) can be applied for the point-to-point RF power transmission system and the space power satellite (SPS). Because of high transmission loss, the efficient energy conversion of the rectenna is the most important portion in the design of the rectenna system.

Two kinds of design technologies are considered for the efficient power conversion. One is how to excite high microwave power into a rectifying diode, and the other is how to increase the rectifying efficiency. For some time, antenna arrays [21]-[22], circularly polarized antennas [22]-[23], and broadband antennas [24] have been used for combining relatively high RF power from the free space. Antenna arrays can increase incident power delivered to a rectifying circuit by increasing the system gain. Circularly polarized antennas can be used to provide radiated power with less polarization mismatches. Broadband antennas have been used for receiving various RF sources to generate higher DC power. For the purpose of increasing the conversion efficiency, several components are required in a rectifying circuit. Because the efficiency of the rectenna is strongly dependent on re-radiated power of harmonic signals generated by a nonlinear diode as well as a fundamental signal, antenna matching circuits and a BPF have been used between the antenna and the diode. In addition, a LPF for a DC path is needed to block RF power leakage into the resistive load.
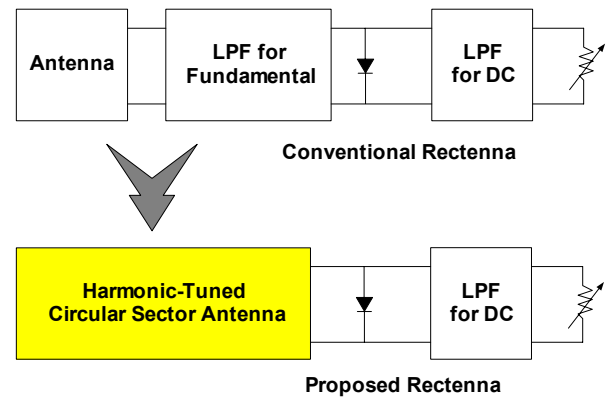
Fig. 9 Block diagram of the conventional and the proposed rectenna system based on the active integrated antenna.

The concept of the active integrated antenna is introduced to design of an efficient rectenna. Under this concept, the antenna provides an additional function such as harmonic rejection in this case. Therefore, the matching circuits and the BPF are not needed for the proposed design as shown in Fig. 9. Since a circular sector antenna in the rectenna can suppress the 2nd and 3rd harmonics, when it is fed at a specific angle along the periphery, the harmonic rejection BPF can be removed. Moreover, the impedance of the rectifying circuit is matched to the input impedance of the circular sector antenna using a coaxial feeding without matching circuits.

B. Circuit Design and Experimental Results

It was verified that the circular sector antenna fed along a 30-degree line provides harmonic rejection properties. However the impedance of the circular sector antenna shows high impedance of over 300 Ω. Therefore, various matching techniques are required such as an inset-feeding. Two kinds of feeding structures such as a planar feedline and a coaxial feedline are designed. In order to avoid radiating the second and the third harmonics from the antenna, a microstrip circular sector antenna with a circular sector angle of 240° and a feeding angle of 30° from the edge of the circular sector is introduced. Because of the circular structure, the higher order resonances are not harmonically related. In addition, due to high impedance of the antenna, an inset feeding method with a quarter-wave length transformer is used for the impedance matching at 2.4 GHz. In order to compare the performance of the antenna, a conventional microstrip square patch antenna is designed at the same resonance frequency. The gain of the circular sector antenna is 4.677 dBi, while that of the square patch antenna is 2.677 dBi. Since a nonlinear diode creates harmonics such as 4.8 GHz and 7.2 GHz, the circular sector antenna is effectively used to block them from re-radiation. The return losses at the second and the third harmonics of the circular sector antenna are very high as seen from Fig. 10.

Furthermore, we investigate another exciting mechanism using a coaxial feeding from the ground plane side, while the harmonic rejection capacity is retained. Fig. 11 illustrates the input impedance of this feeding mechanism versus the distance, d from the center point of the antenna. The antenna with a 50-Ω

input impedance is designed at a frequency of 2.4 GHz. The feeding point is at d = 110 mils from the center of the antenna on a substrate with a dielectric constant of 2.33 and thickness of 31 mils. The radius of 780 mils and the sector angle of 120 degrees are chosen.
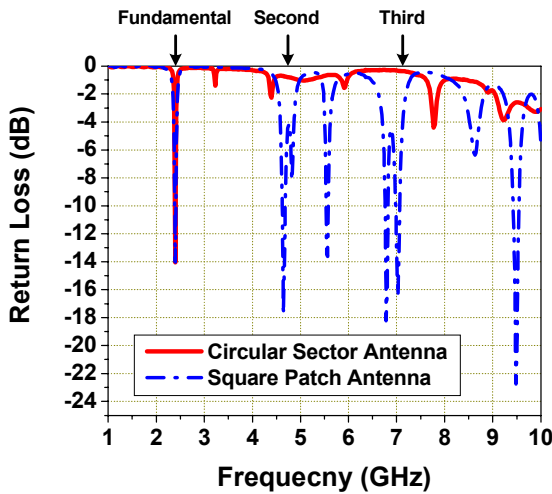
Fig. 10 Measured return losses of the microstrip circular sector and square patch antennas.
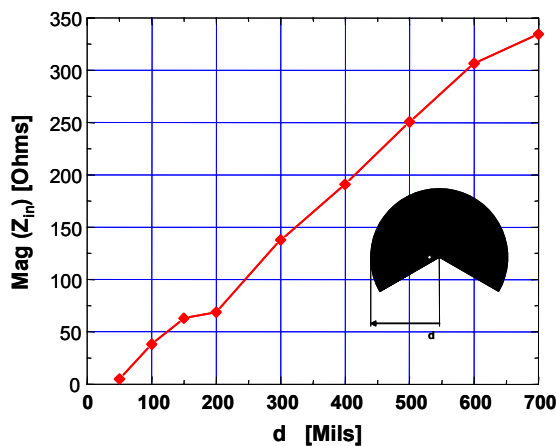
Fig. 11 Antenna input impedance of the coaxial-fed circular sector antenna as a function of the distance from the center of the antenna.
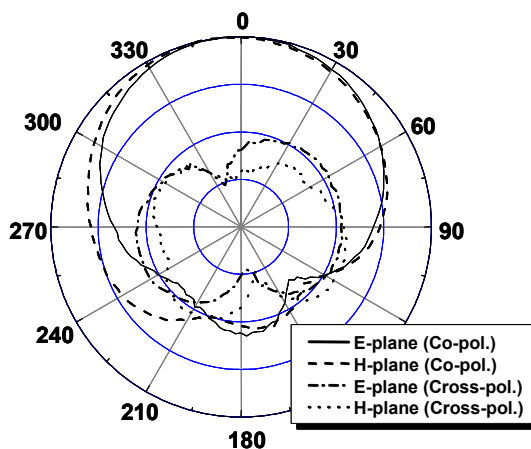
Fig. 12 Radiation patterns of the coaxial-fed circular sector antenna.

As a result, harmonic powers generated from a rectifying diode can be re-used for increasing the overall efficiency without a BPF. The radiation patterns of the antenna are typical ones of a patch antenna. The gain of this antenna is found to be 6.33 dBi. Although its feeding point is near the center, the antenna has linear polarization and low cross polarization level of less than 20 dB as shown in Fig. 12. The proposed rectennas with the two kinds of circular sector antennas are depicted in Fig. 13. The rectifying circuit consists of a rectifying diode, a LPF, and a load resistor. The RF Schottky barrier detector diode (HSMS-2820) is mounted on the input port of the microstrip LPF. The LPF is designed as a DC path and a blocker for fundamental and 2nd & 3rd harmonic signals. The rectifying circuit is directly connected on the back side of the circular sector antenna via hole.

The efficiency of the proposed rectenna is measured for various resistive loads from 100 Ω to 250 Ω. In general, the overall efficiency of a rectenna is defined as the ratio of dc power to incident RF power as below [20].

$$\eta_o = \frac{dc\ output\ power}{incident\ RF\ power} = \frac{V^2/R_{Load}}{P_A} \qquad (2)$$
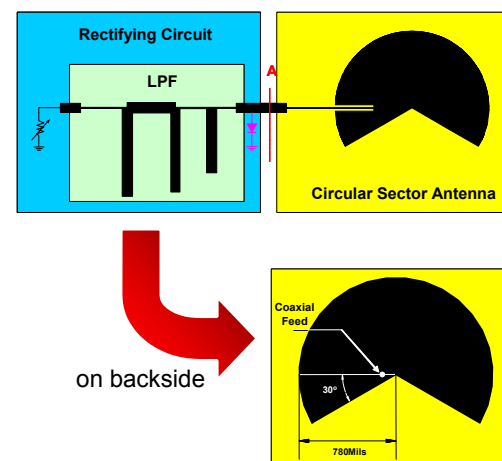
Fig. 13 Rectenna layouts with the coaxial-fed circular sector antenna fed either a planar feedline or a coaxial feedline from back side.

The applied input RF power is measured using the same antenna without the rectifying circuit. Fig. 14 illustrates the efficiency of the rectenna with the planar-fed circular sector antenna as a function of the input power at A for the various resistor loads. Four resistor values are selected, which are 100, 150, 200, and 250 Ω. Based on the data sheet of the diode, up to saturation input power of +10 dBm is applied. As the input power is increased, efficiency is also increased. A maximum efficiency of 77.8% is achieved with the load resistor of 150 Ω when input power is 10 dBm. For the coaxial-fed antenna, it makes a maximum efficiency of 56.7% at a 150-Ω load, which is relatively lower value. It is the reason why the coaxial-fed antenna has no matching circuit like an inset-feeing and a

transformer using a narrow microstrip line in the planar-fed structure. By using the simple matching circuit between the antenna and the rectifying circuit, it achieves a maximum efficiency of up to 80 %.

The proposed rectenna has less complexity due to use of a circular sector antenna that has a built-in harmonic rejection property. It can be designed without a BPF. The use of a coaxial feeding would provide an additional advantage that all low frequency circuit is separated from the antenna surface.
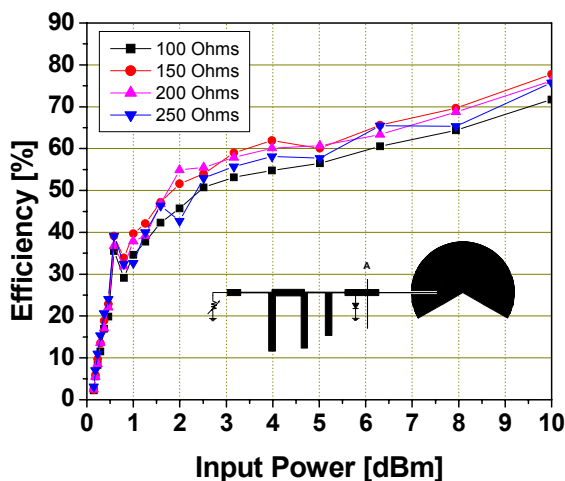
Fig. 14 Overall efficiency of the proposed rectenna with the planar-fed circular sector antenna as a function of the input power at point A.

IV. CONCLUDING REMARKS

As presented above, the AIA is an interesting subject for advanced RF front-end systems. In this paper, two AIA systems using a circular sector antenna, which characterizes the harmonic rejection, are presented. The power amplifier and rectenna design based on the AIA concept has been shown to provide an efficient and successful method for designing high efficiency and compact systems. It can eliminate filters or terminations which cause insertion loss for the fundamental frequency. With the solid-state devices, integrated circuits as well as the novel fabrication technologies such as microelectromechanical systems (MEMS), the novel design technologies based on the AIA concept are expected to lead the innovated system by merging in the coming years.

REFERENCES

[1]   K. Chang, R. A. York, P. S. Hall, and T. Itoh, "Active Integrated Antennas," *IEEE Trans. Microwave Theory Tech.*, vol. 50, pp. 937-944, March 2002.

[2]   N. Kaneda, W. R. Deal, Y. Qian, R. Waterhouse, and T. Itoh, "A broadband planar quasi-Yagi antenna," *IEEE Trans. Antenna and Propaga.*, vol. 50, pp. 1158-1160, Aug. 2002.

[3]   C. Y. Hang, W. R. Deal, Y. Qian, and T. Itoh, "High-efficiency push-pull power amplifier integrated with quasi-Yagi antenna," *IEEE Trans. Microwave Theory Tech.*, vol. 49, pp. 1155-1161, June 2001.

[4]   S. Lin, Y. Qian, and T. Itoh, "A low noise active integrated antenna receiver for monopulse radar applications," *IEEE MTT-S Int. Microwave Symp. Dig.*, May 2001, pp. 1395-1398.

[5]   M. Sironen, Y. Qian, and T. Itoh, "A subharmonic self-oscillating mixer with integrated antenna for 60 GHz wireless applications," *IEEE Trans. Microwave Theory Tech.* vol. 49, pp. 442-450, March 2001.

[6]   Y. Chung, C. Y. Hang, S. Cai, Y. Qian, C. P.Wen, K. L. Wang, and T. Itoh, "AlGaN/GaN HFET Power Amplifier Integrated with Microwtrip Antenna for RF Front-End Applications," *IEEE Trans. Microwave Theory Tech.*, vol. 51, pp. 653-659, Feb. 2003.

[7]   V. Radisic, Y. Qian, and T. Itoh, "Class F power amplifier integrated with circular sector microstrip antenna," *IEEE MTT-S Int. Microwave Symp. Dig.*, June 1997, pp. 687-690.

[8]   W. F. Richards, J. D. Ou, and S. A. Long, "A theoretical and experimental investigation of annular, annular sector, and circular sector microstrip antennas," *IEEE Trans. Antennas Propagat.*, vol. 32, pp. 864–867, Aug. 1984.

[9]   J.-Y. Park, S.-M. Han, and T. Itoh, "A rectenna design with harmonic- rejecting circular sector antenna," *IEEE Antennas Wireless Progagat. Lett.*. vol. 3, pp. 52-54, 2004.

[10] S.-M. Han, J.-Y. Park, and T. Itoh, "Active Integrated Antenna Based Rectenna Using the Circular Sector Antenna with Harmonic Rejection," *2004 IEEE AP-S Int. Symp. Dig.,* June 2004, pp. 3533-3536.

[11] S. C. Cripps, *RF power amplifiers for wireless communications*, Norwood, MA: Artech House, 1999.

[12] D. M. Snider "A theoretical analysis and experimental confirmation of the optimally loaded and overdrive RF power amplifier", *IEEE Trans. Electron Devices,* vol. 14, No. 12, pp. 851-857, 1967.

[13] W.S. Kopp, S. D. Pritchette, "High efficiency power amplification for microwave and millimeter frequencies," *IEEE MTT-S Int. Microwave Symp. Dig.,* vol. 3, pp. 857-858, 1989.

[14] I. J. Bahl, E. L. Griffin, A. E. Geissberger, C. Andricos, and T. F. Brukiewa, "Class-B power MMIC amplifiers with 70 percent power-added efficiency," *IEEE Trans. Microwave Theory Tech.,* vol. 37, No. 9, pp. 1315-1320, 1989.

[15] W. R. Deal, V. Radisic, Y. Qian, and T. Itoh, "Integrated-antenna push-pull power amplifiers," *IEEE Trans. Microwave Theory Tech.*, vol. 47, No. 8, pp. 1418-1425, 1999.

[16] V. Radisic, Y. Qian, and T. Itoh, "Novel architectures for high-efficiency amplifiers for wireless applications," *IEEE Trans. Microwave Theory Tech.*, vol. 46, No. 11, pp. 1901-1909, 1998.

[17] Y. Takayama, "A new load-pull characterization method for microwave power transistors," *IEEE MTT-S Int. Microwave Symp. Dig.*, pp. 218-220, 1976.

[18] Y. Ohno, and M. Kuzuhara, "Application of GaN-based heterojunction FETs for advanced wireless communication," *IEEE Trans. Electron Devices*, vol. 48, No. 3, pp. 517-523, 2001.

[19] W. C. Brown, "The History of Power Transmission by Radio Waves," *IEEE Trans. Microwave Theory Tech.*, vol. MTT-32, pp. 1230-1242, Sep. 1984.

[20] J. O. McSpadden, L. Fan, and K. Chang, "Design and Experiments of a High-Conversion Efficiency 5.8-GHz Rectenna," *IEEE Trans. Microwave Theory Tech.*, vol. 46, pp. 2053-2060, Dec. 1998.

[21] N. Shinohara and H. Matsumoto, "Experimental study of large rectenna array for microwave energy transmission," *IEEE Trans. Microwave Theory Tech.*, vol. MTT-46, pp. 261-268, March 1998.

[22] B. Strassner and K. Chang "5.8-GHz circularly polarized dual-rhombic-loop traveling-wave rectifying antenna for low power-density wireless power transmission applications", *IEEE*

Trans. Microwave Theory Tech., vol. MTT-51, pp. 1548-1553, May 2003.

[23] Y.-H. Suh, C. Wang, and K. Chang, "Circularly polarized truncated-corner square patch microstrip rectenna for wireless power transmission," *Electrion. Lett.*, vol. 36, pp. 600-602,

March 2000.

[24] J. A. Hagerty and Z. Popovic, "An experimental and theoretical characterization of a broadband arbitrarily-polarized rectenna Array," *IEEE MTT-S Int. Microwave Symp. Dig.*, vol. 3 June 2001, pp. 1855-1858